The Ohio State University: College of Biomedical Engineering

Undergraduate Honors Research Thesis

Mitochondrial Calcium Changes in Sheared Human Vascular Endothelial Cells

By Thomas Esber

Primary Investigator: Dr. B. Alevriadou, PhD

Co-Adviser: Mark Ruegsegger, PhD

Laboratory Supervisor: Akshar Patel, PhD candidate

Abstract

Endothelial cells are subjected to various forces and stresses causing physiological reactions to occur. Changes in cytosolic and mitochondrial calcium due to shear forces/stresses are required to maintain homeostasis of the cell. Monitoring these changes are vital to scientific research and are done using fluorophores. Human umbilical vein endothelial cells (HUVECs) were subjected to two fluorophores with different excitation and emission wavelengths, Fluo-4 and Rhod-2. While examining collected data, it was noted that during a static baseline recording, premature excitation of Fluo-4 fluorescence was being experienced by some cells. The cause of this excitation was phototoxicity, a result of light exposure. A static baseline was conducted using only Fluo-4 in which no phototoxicity was experienced. An experiment was then analyzed using *MATLAB* comparing the fluorescence over time in cells that used both Fluo-4 and Rhod-2. It was shown that early fluorescence was occurring in multiple cells as well as an overall decrease in fluorescence over time, indicating photobleaching. These results indicated that Rhod-2 was causing the photoactivation of fluorophores. Previous studies potentially explain the mechanism to be an increase in radical oxidative species (ROS) which activate the inositol 1,4,5-trisphosphate receptor. Further studies will be conducted without the use of Rhod-2 and instead will use an adenovirus to transfect cells.

Key words: Endothelial Cells, HUVECs Rhod-2, Fluo-4, Photoactivation, Phototoxicity, IP_3R, Calcium

Table of Contents:

Introduction

Endothelial cells (ECs) are constantly impacted by localized mechanical forces, including shearing forces/shear stresses from blood flow on their apical surface.[1] These cells undergo physiological responses such as dynamic changes in the concentration of intracellular calcium ions ($[Ca^{2+}]_i$). Cells are highly dependent on Ca^{2+} ions channels, as well as sodium, potassium, and chloride in order to regulate Ca^{2+} into and out of the organelles (specifically the endoplasmic reticulum, ER, and mitochondria). As a result, cell function and health are maintained in homeostasis.[2] This is especially true for the inositol 1,4,5-trisphosphate receptor (IP_3R) that is responsible for releasing Ca^{2+} from the ER into the cytosol following stimulation by IP_3 and/or low concentrations of $[Ca^{2+}]_i$. Previously, our lab showed that oscillatory changes in $[Ca^{2+}]_i$ are also regulated by Ca^{2+} being transported in and out of the mitochondria, the second largest store of Ca^{2+} in the cell.[3] These oscillation changes are normal and maintain homeostasis in the cell but can become dysfunctional if the oscillations become irregular or overly frequent. On the mitochondrial inner membrane, there is a Ca^{2+} channel called the Mitochondrial Calcium Uniporter (MCU), which is the major channel for Ca^{2+} uptake from the cytosol into the mitochondria.

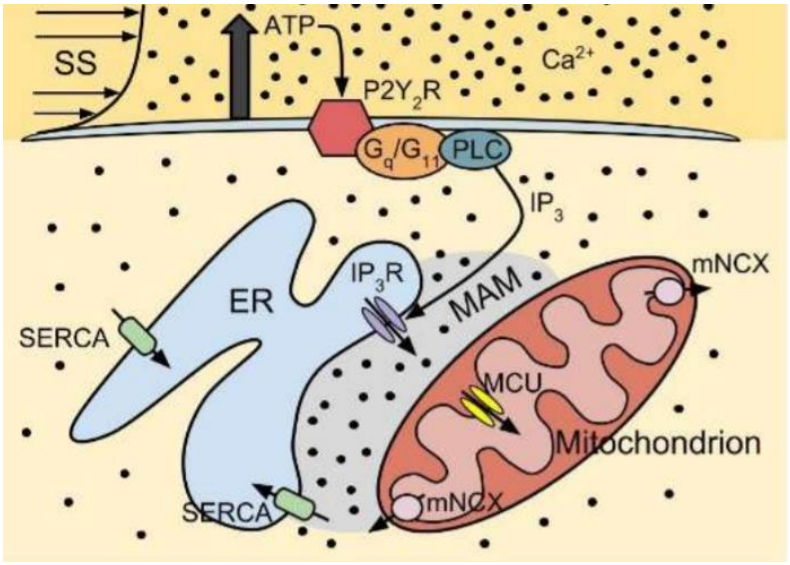

Fig. 1: The oscillatory $[Ca^{2+}]_i$ response in sheared ECs depends on healthy mitochondria that can uptake (and release) Ca^{2+} via the MCU (and mNCX). The IP_3R stimulation and its function is also shown in the diagram.

ECs are also impacted by radical oxidative species (ROS). These molecules are byproducts of oxidative reactions and are known to cause dysfunction, leading to narrowing of the vascular walls and plaque buildup, which are fundamental signs of atherosclerosis. ROS directly impacts the proteins that are associated with Ca^{2+} oscillations such as the MCU and IP_3R and can activate these proteins due to oxidative binding.

In an attempt to record Ca^{2+} changes in both the cytosol and mitochondria in ECs during perfusion testing, two fluorescent dyes were used: Fluo-4 and rhodamine-2 (Rhod-2), respectively. Each fluorescent stain has a respective excitation and emission wavelength range as seen in Figure 2.

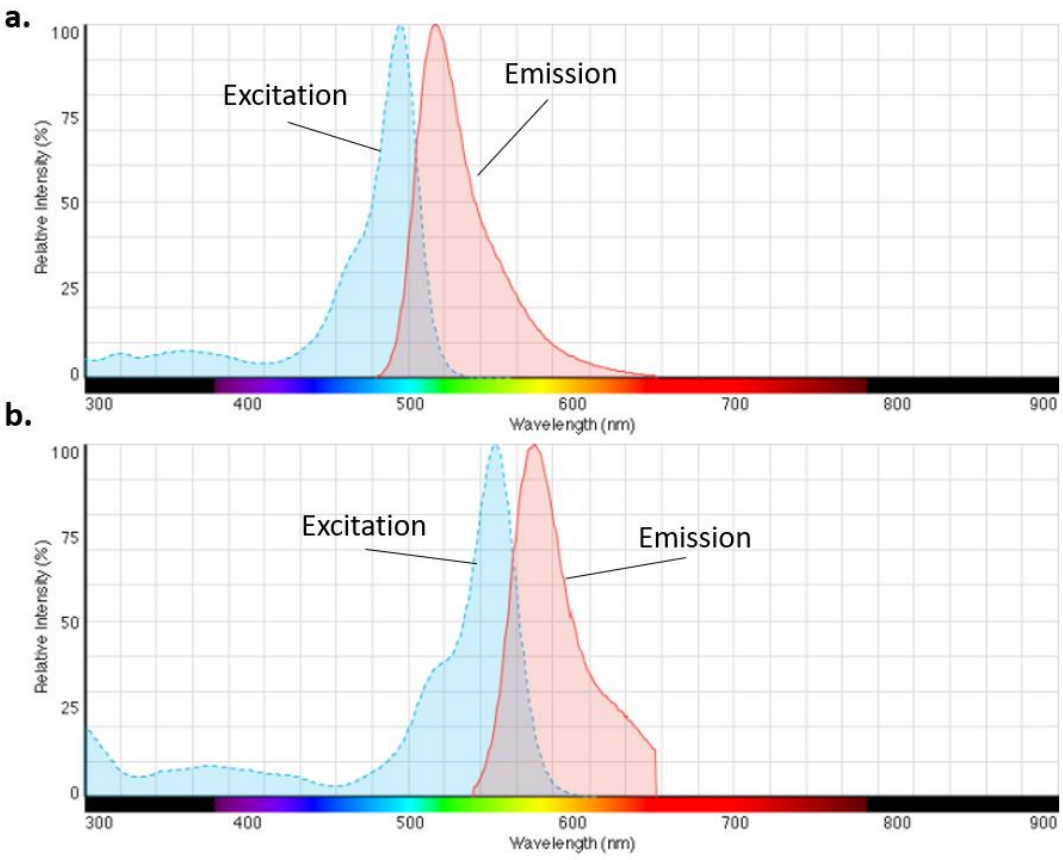

Fig. 2: **(a)** Wavelength of excitation and emission for Fluo-4 **(b)** Wavelength of excitation and emission of Rhod-2 Figures were obtained from Thermo Fisher Scientific®

Under microscopic observations, the baseline measurement (a 1-minute static period to monitor the cells' lack of change in fluorescence) of Fluo-4 fluorescence proved to be problematic due to obvious changes in fluorescence. A suspected reason for this occurrence was phototoxicity, a generalized term for any light damage that a cell undergoes from light exposure.[4] Ultimately, phototoxicity cannot be eliminated due to inherent light exposure to the cells. However, phototoxicity can be a result of an at-risk cell due to chemical stimulations. The goal of this thesis is to measure both cytosolic and mitochondrial Ca^{2+} by double labeling the ECs and recording the fluorescent changes over time. However, under our experimental conditions, phototoxicity occurred. We ended up showing the direct impact of phototoxicity on fluorescent images, as well as the comparison of good-quality and poor-quality fluorescence data.

Materials and Methods

Human umbilical vein endothelial cells (HUVECs) were obtained at passage 3 and seeded in a Corning® T25 cell culture flask with 10 mL of EGM™ Endothelial Cell Growth Medium BulletKit™. After 2 days, a confluent monolayer was observed, and the cells were split into a Corning® T75 cell culture flask using 20 mL of media. Confluency was once again reached, and the cells were transferred to ibidi® µ-Slide VI 0.4 well slides and allowed to incubate at 37˚ C, 5% CO_2 for 24 hours.

The cell media was replaced with Hank's Balanced Salt Solution (HBSS) and incubated for 40 minutes at 37˚ C. A 1 mM stock Rhod-2 solution was created from 50 µg Rhod-2 and 44.5 µL DMSO. The HBSS on the slides was replaced with the Rhod-2 stain solution (1 µL of stock RHod-2 plus 0.5 µL sulfinpyrazone in 500 µL HBSS), pipetting 200 µL at a time while aspirating all existing HBSS. The last 100 µL of the Rhod-2 stain solution was kept in the slide. The slides were incubated for a following 30 minutes at 37˚ C.

A stock Fluo-4 solution was made using 50 µg of Fluo-4 with 45.6 µL DMSO resulting in a 1 mM Fluo-4 solution. The Rhod-2 stain solution was replaced with the Fluo-4 stain solution (1.5 µL of stock Fluo-4 in 500 µL HBSS) using the same convention mentioned previously and incubation lasted for 20 minutes. The Fluo-4 stain solution was replaced with HBSS and the slide was loaded onto the microscope.

Using a Nikon epifluorescence microscope and a CCD camera, the slides were imaged at 40 x and digital images were acquired with *Nikon Elements* software. A glass syringe and Harvard Apparatus 11 Pico Plus Elite Syringe Pump was used to perfuse HBSS over the cells. A simple program was created that observed the fluorescence baseline of the cells for 1 minutes

followed by perfusion of HBSS at a flow rate corresponding to 10 dynes/cm^2 shear stress for 4 minutes. The flow was stopped for the remaining 2 minutes of the test. Throughout this time, alternating images of the cells are being taken using a green and red filter to detect the Fluo-4 and Rhod-2 fluorescence respectively. Fluo-4 emission and excitation were taken using an FITC HQ (Excitation: 460-500nm, Emission 510-560nm, Dichroic Mirror: 505nm) and Rhod-2 emission and excitation were obtained using a CY3 HQ (Excitation 530-560nm, Emission: 573-648, Dichroic Mirror: 570nm). Images were stored in *Nikon Elements* and further analyzed.

The compiled videos of the cells were set to the dimension of 640 x 512 pixels and saved as an AVI file. Using *ImageJ*, a stack z-projection was taken of the image and analyzed through *Cell Profiler* to find the outlines of the cells. *MATLAB* was then able to identify these outlined regions and was utilized to find the necessary individual pixel within the cells. Each pixel intensity was then recorded and averaged over the cell to record each cell's fluorescence over time. This process was performed for a static control that experiences no flow exposure and for an experiment with both Rhod-2 and Fluo-4, revealing both red and green fluorescence.

Results

An initial test was run using Fluo-4 to verify that a steady baseline is achievable in the presence of a single fluorophore when the cells are kept under static conditions. Fluorescence baseline data are shown in Figure 3. Cells #2 and #4 are displayed and show a baseline of approximately zero normalized fluorescence, which is directly proportional to $[Ca^{2+}]_i$. It is to be noted that fluctuations in the data are due to noise during data collection. This was determined by the average normalized fluorescence being 0.055±0.080 and 0.085±0.089 for Cells #2 and #4 respectively over a time period of 287 seconds.

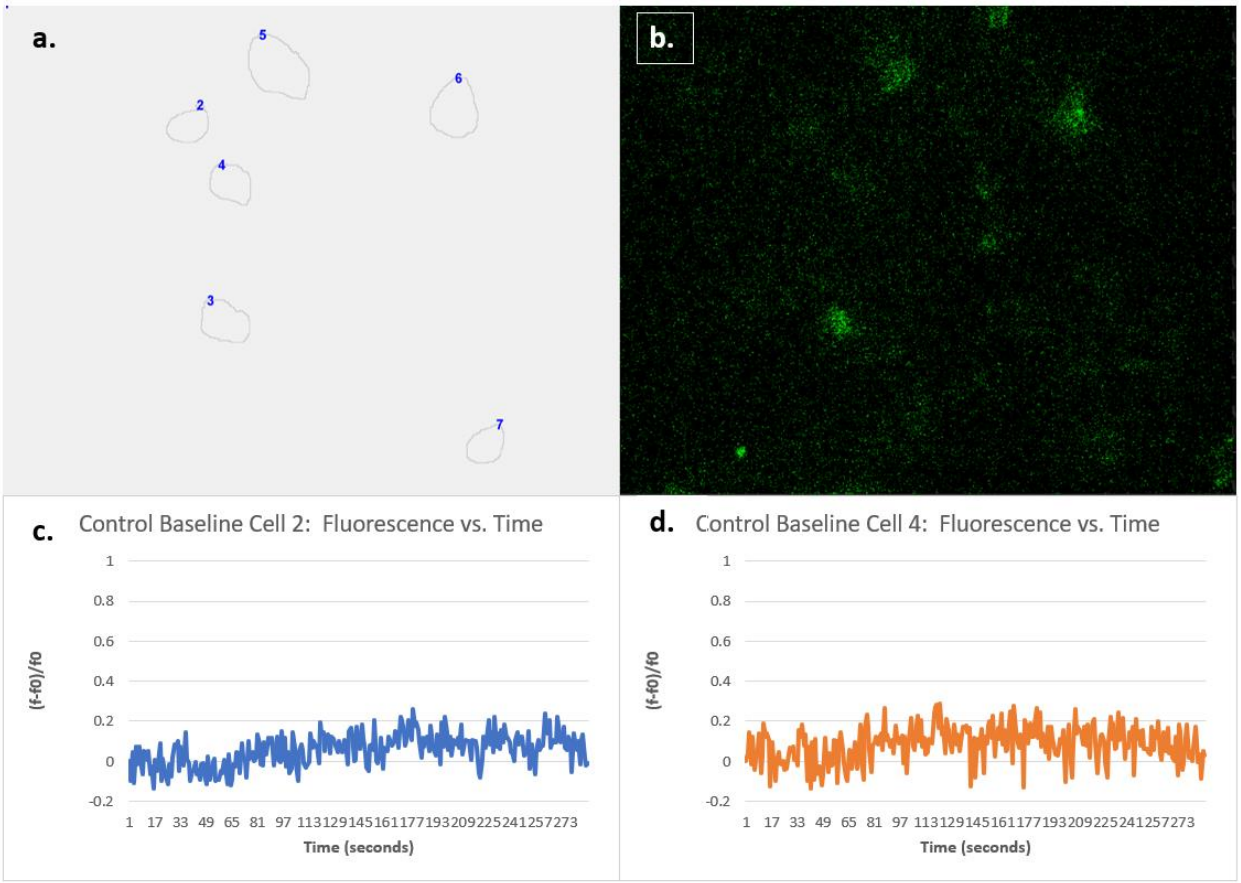

Fig. 3: **(a)** Cellular outline using *Cell Profiler*. **(b)** HUVEC cells after Fluo-4 stain at 20x magnification. **(c)** Normalized fluorescence data over 287 seconds for Cell #2 according to Figure 3a. **(d)** Normalized fluorescence data over 287 seconds for Cell #4 according to Figure 3a.

During flow testing, both red and green fluorescence was observed. Some cells (i.e. Cells #9 and #11) experienced the expected behavior of a relatively flat baseline and of $[Ca^{2+}]_i$ oscillations starting at 60 seconds (the start of the flow of 10 dynes/cm^2). A large peak of fluorescence was observed through both red and green filters as well as continued oscillations. In Cell #11, oscillations were shown to decrease in magnitude until flow was stopped at time t=300 seconds.

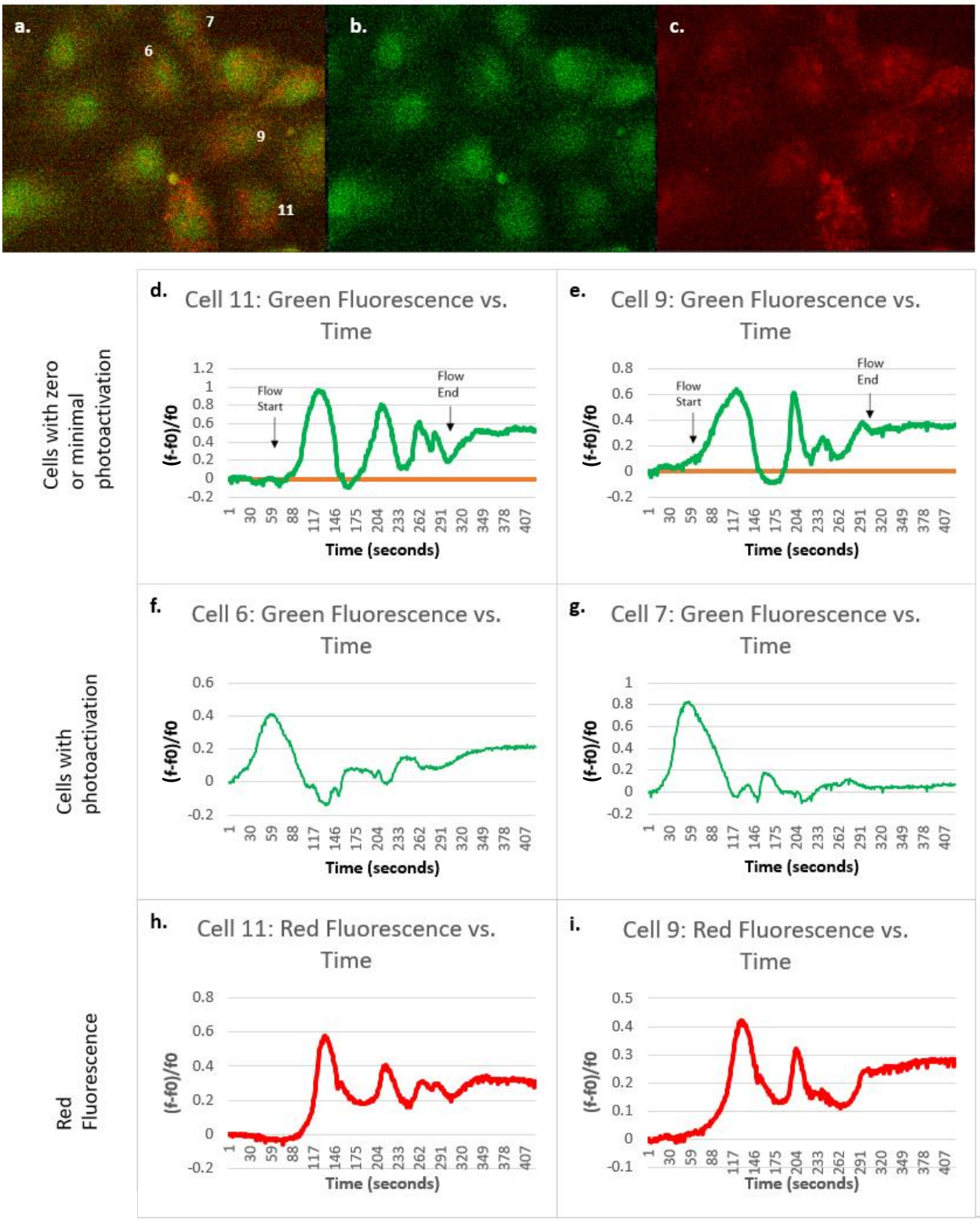

Fig. 4: **(a)** Combined fluorescence image and cell number labels. **(b)** Green fluorescence. **(c)** Red fluorescence. **(d)** Normalized green fluorescence for Cell #11. **(e)** Normalized green fluorescence for Cell #9. **(f)** Normalized green fluorescence for Cell #6. **(g)** Normalized green fluorescence for Cell #7. **(h)** Normalized red fluorescence for Cell #11. **(d)** Normalized red fluorescence for Cell #9.

However, multiple cells in the same microscope field of view experienced premature activation of Fluo-4 during the 1-minute baseline. These cells started to fluoresce before any flow was started. Cells, such as Cells #6 and #7, experienced the initial fluorescence peak and proceeded to decrease in signal, eventually having irregular patterns or a minimalized signal before the end of the flow test. Furthermore, almost all cells had elevated green fluorescence levels during the last 2 minutes of the experiment when the flow was completely stopped.

Rhod-2, which tends to concentrate in the mitochondria, was effective in showing red fluorescence within the mitochondrial network. This can clearly be seen in Figure 1c. It was also shown that mitochondrial Ca^{2+} concentration ($[Ca^{2+}]_m$), measured by the red fluorescence, was increasing and decreasing in synchronization with the $[Ca^{2+}]_i$, measured by the green fluorescence.

Discussion

When the ECs were loaded by both Fluo-4 and Rhod-2 (each at the final concentrations of 2 μm) we observed activation of the fluorophores during the baseline, which indicates cell photoactivation. This photoactivation was not shown in every cell in each image and was absent when the ECs were loaded with only Fluo-4. This indicates that Rhod-2 may be impacting Ca^{2+} fluctuations in the cells due to underlying physiological reactions. Key players in Ca^{2+} homeostasis are the ER and mitochondria, as previously mentioned. The ER is the largest Ca^{2+} store in the cell and when signaled (by either shear stress or chemical stimulation), Ca^{2+} is released into the cytosol via the IP_3R which then leads to Ca^{2+} uptake by the mitochondria. This

leads to a series of events that causes both organelles to take in and release Ca^{2+} causing the observed $[Ca^{2+}]_i$ oscillations.[3]

The IP_3R can be activated through multiple means. First, a low $[Ca^{2+}]_i$ activates the IP_3R causing the ER to release more Ca^{2+} through the IP_3R. This mechanism can be inhibited by high $[Ca^{2+}]_i$. The other way the IP_3R can be activated by ROS. ROS are products of oxidation reactions inside the cell and are also majorly produced by the mitochondrial respiratory chain. ROS can then trigger the IP_3R (as well as the MCU and other channels) to be activated, leading to ER Ca^{2+} release.[5]

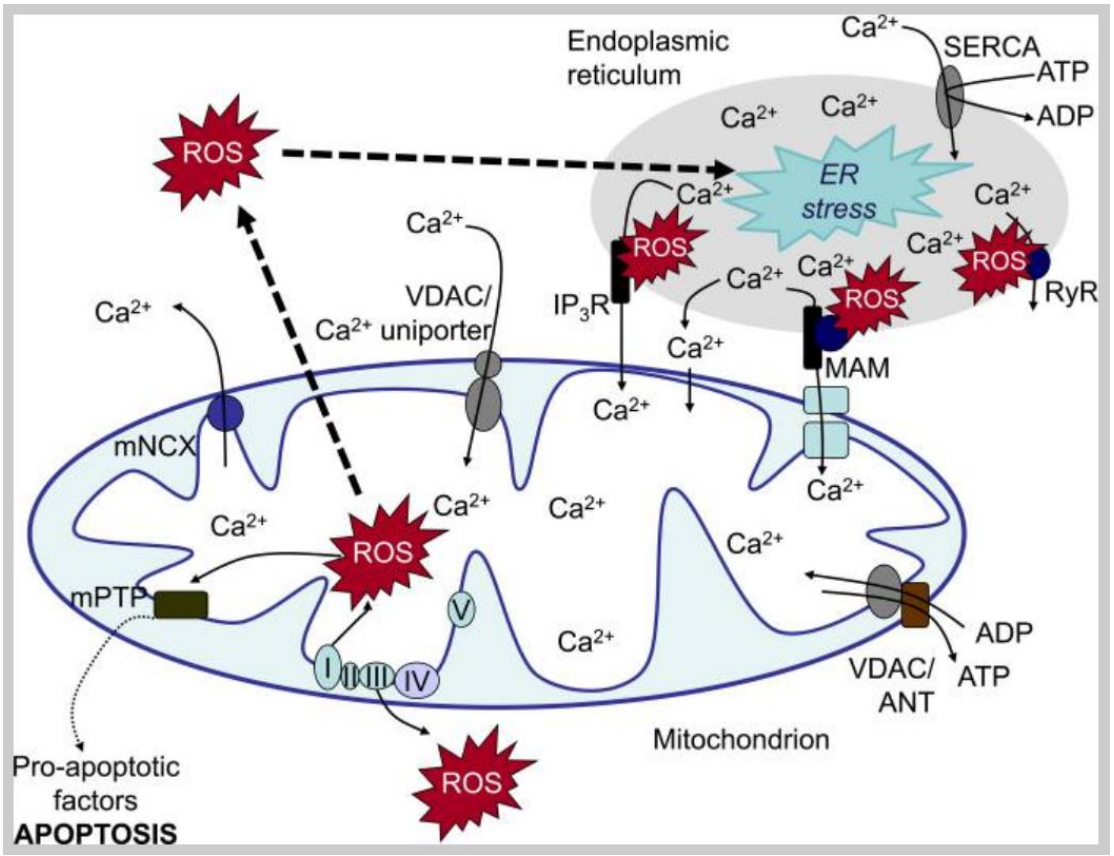

Fig. 5: ROS interplay between the mitochondria and endoplasmic reticulum. This figure shows how ROS is produced and can impact the IP_3R as well as leave the mitochondria to disturb other homeostatic processes. Figure obtained from Görlach A. 2015.

Potential phototoxicity due to Rhod-2 can explain why baseline activation of Fluo-4 (and resultant Ca^{2+} oscillations) occurred. The significant spike in Fluo-4 fluorescence experienced in some cells was most likely due ROS-mediated activation of the IP_3R following the presence of Rhod-2 in the mitochondria. An indicator of photoactivation is autofluorescence, meaning fluorophore activation occurs without any noted stimulus. This may also be a marker of photodamage in the cell.[6] This only occurred when Rhod-2 was in the cells and was noted due to having green fluorescence observed earlier than expected. Autofluorescence was also seen at the final phase of the experiment. The cells were not subjected to any flow during the last two minutes but continued to have a steady fluorescence. Ca^{2+} oscillations were still occurring due to activation of the key proteins that regulate this process, indicating ROS stimulation of the proteins. Furthermore, photobleaching is a significant indicator of phototoxicity. Fluorophores are damaged due to light and can no longer produce fluorescence.[4] This was directly observed in some cells. The fluorescence observations showed that the oscillation peaks experienced dampening over time or completely disappeared before the flow was stopped.

Steps were taken to decrease phototoxicity risks in our experiments. First, the concentration of Rhod-2 was decreased to 1 μM to limit toxic effects on the cell. Moreover, the light exposure that was used for both red and green excitation was set to the lowest possible setting that the lamp source could allow. If the setting was lowered any more, images would not be recordable. Minimizing the intensity of the excitation limits the exposure to light and therefore phototoxicity. These changes in parameters did not change cellular Ca^{2+} excitation, further indicating chemical stimulations occurring inside the cell.

The data recorded had both positive and negative qualities. Ca^{2+} fluctuations were recorded in both the cytosol and mitochondria using red and green filters. Also, stalled

oscillations between the cytosol and mitochondria were successfully observed. These successes are crucial for future studies and will allow for further experiments on Ca^{2+} concentration measurements. Contrarily, a direct quantification of ROS production was not obtained to prove the mechanism for phototoxicity by Rhod-2. All that can be stated at this time is that Rhod-2 impacts Ca^{2+} concentrations without any stimulus. For future work, Fluo-4 will continue to be used, but a new way to observe $[Ca^{2+}]_m$ will need to be explored. Adenoviruses have a high transfection rate and have been highly tested. The incorporation of a gene, that expresses a fluorophore, into the host's genome also decreases the chances of chemical stimulations. If this method was used, a new procedure for cell incubation would need to be created due to the time (at least 24 hours) the virus takes to incorporate into the host's genome and for the protein to be expressed.

Conclusion

Cellular concentrations of Ca^{2+} is a necessary and vital component for controlling cellular homeostasis. Imbalances in this ion can lead to dysfunction due to ROS production, eventually leading to macroscopic complications. Recording Ca^{2+} changes in the cell, in both the cytosol and mitochondria, is important and having real-time data to show how these two locations' concentrations interplay can help explain potential mechanisms. However, photoactivation (as well as ROS production) of fluorophores can impact data collection due to resulting premature activations as well as photobleaching. Future work should further investigate this mechanism of chemical stimulation in order to better understand cellular function and to prevent the use of those stains which may cause side effects and generate erroneous data.

Acknowledgements

I personally want to thank Dr. Barbara Alevriadou and Akshar Patel for the time they have taken to incorporate me into the Vascular Mechanotransduction and Oxidative Stress laboratory. Their guidance has taught me lessons in research, academia, and professionalism. I would also like to thank the College of Biomedical Engineering at The Ohio State University for the education that I have received and for helping me accomplish my life goals. The past four years at this university has set me on my career path and the teachings that I have gained here will continue to push me in my future work in the scientific community.

References:

1. Davies PF, Civelek M, Fang Y, Fleming I. The atherosusceptible endothelium: endothelial phenotypes in complex hemodynamic shear stress regions in vivo. Cardiovasc Res. 2013;99(2):315-27.

2. Gerhold KA, Schwartz MA. Ion Channels in Endothelial Responses to Fluid Shear Stress. Physiology (Bethesda). 2016;31(5):359-69.

3. Scheitlin CG, Julian JA, Shanmughapriya S, Madesh M, Tsoukias NM, Alevriadou BR. Endothelial mitochondria regulate the intracellular Ca2+ response to fluid shear stress. Am J Physiol-Cell Physiol. 2016;310(6):C479-90.

4. Laissue PP, Alghamdi RA, Tomancak P, Reynaud EG, Shroff H. Assessing phototoxicity in live fluorescence imaging. Nature methods. 2017 Jun 29;14(7):657.

5. Görlach A, Bertram K, Hudecova S, Krizanova O. Calcium and ROS: a mutual interplay. Redox biology. 2015 Dec 1;6:260-71.

6. Uckermann O, Galli R, Tamosaityte S, Leipnitz E, Geiger KD, Schackert G, Koch E, Steiner G, Kirsch M. Label-free delineation of brain tumors by coherent anti-stokes Raman scattering microscopy in an orthotopic mouse model and human glioblastoma. PLoS One. 2014 Sep 8;9(9):e107115.